Magnetohydrodynamic description of plasmas

Part III

Daniel Gómez [1,2]

Group of Astrophysical Flows
Buenos Aires - Argentina

Email: gomez@iafe.uba.ar Webpage: http://astro.df.uba.ar

(1) Instituto de Astronomía y Física del Espacio, CONICET-UBA, Argentina
(2) Departamento de Física, Fac. Cs. Exactas y Naturales, UBA, Argentina

ICTP-IAEA College on Plasma Physics, November 18, 2016

Small scales: multi-species plasmas

- Even though at large scales, one-fluid MHD is a reasonable description, a two-fluid model brings new physics into play, with the corresponding spatial (and temporal) scales.
- For each species s we have (Goldston & Rutherford 1995):
  - Mass conservation $$\frac{\partial n_s}{\partial t} + \vec{\nabla} \cdot (n_s \vec{U}_s) = 0$$
  - Equation of motion $$m_s n_s \frac{d\vec{U}_s}{dt} = q_s n_s (\vec{E} + \frac{1}{c} \vec{U}_s \times \vec{B}) - \vec{\nabla} p_s + \vec{\nabla} \bullet \vec{\sigma}_s + \sum_{s'} \vec{R}_{ss'}$$
  - Momentum exchange rate $$\vec{R}_{ss'} = -m_s n_s \upsilon_{ss'} (\vec{U}_s - \vec{U}_{s'})$$
- These moving charges act as sources for electric and magnetic fields:
  - Charge density $$\rho_c = \sum_s q_s n_s \approx 0$$
  - Electric current density $$\vec{J} = \frac{c}{4\pi} \vec{\nabla} \times \vec{B} = \sum_s q_s n_s \vec{U}_s$$
- In the incompressible limit: $n_s = 0$ $\quad$ $\vec{\nabla} . \vec{U}_s = 0$

Small scales: EIHMHD equations

- The dimensionless version, for a length scale L_0, density n_0 and Alfven speed $v_A = B_0 / \sqrt{4\pi m_i n_0}$

$$\boxed{\begin{aligned} \frac{d\vec{U}_i}{dt} &= \frac{1}{\varepsilon}(\vec{E} + \vec{U}_i \times \vec{B}) - \frac{\beta}{n}\vec{\nabla}p_i - \frac{\eta}{\varepsilon n}\vec{J} \\ \frac{m_e}{m_i}\frac{d\vec{U}_e}{dt} &= -\frac{1}{\varepsilon}(\vec{E} + \vec{U}_e \times \vec{B}) - \frac{\beta}{n}\vec{\nabla}p_e + \frac{\eta}{\varepsilon n}\vec{J} \qquad \text{where} \qquad \vec{J} = \vec{\nabla} \times \vec{B} = \frac{n}{\varepsilon}(\vec{U}_i - \vec{U}_e) \end{aligned}}$$

- We define the Hall parameter $\varepsilon = \dfrac{c}{\omega_{pi} L_0}$

as well as the plasma *beta* $\beta = \dfrac{p_0}{m_i n_0 v_A^2}$ and the electric resistivity $\eta = \dfrac{c^2 \nu_{ie}}{\omega_{pi}^2 L_0 v_A}$

- Adding these two equations yields:

$$\boxed{\frac{d\vec{U}}{dt} = (\vec{\nabla} \times \vec{B}) \times (\vec{B} + \varepsilon_e^2 \vec{\nabla} \times \vec{J}) - \vec{\nabla} p}$$

where $\vec{U} = \dfrac{m_i \vec{U}_i + m_e \vec{U}_e}{m_i + m_e}$

and $p = p_i + p_e$

$$\varepsilon_e = \sqrt{\frac{m_e}{m_i}}\,\varepsilon = \frac{c}{\omega_{pe} L_0}$$

Retaining electron inertia: EIHMHD equations

- In the equation for electrons (assuming incompressibility)

$$\frac{m_e}{m_i}\frac{d\vec{U}_e}{dt} = -\frac{1}{\varepsilon}(\vec{E} + \vec{U}_e \times \vec{B}) - \beta_e \vec{\nabla} p_e + \frac{\eta}{\varepsilon}\vec{J} \qquad \vec{J} = \vec{\nabla}\times\vec{B} = \frac{1}{\varepsilon}(\vec{U}_i - \vec{U}_e)$$

we replace $\vec{E} = -\frac{1}{c}\frac{\partial \vec{A}}{\partial t} - \vec{\nabla}\phi \quad and \quad \vec{B} = \vec{\nabla}\times\vec{A}$

to obtain the following generalized induction equation (Andrés et al. 2014ab, PoP)

$$\boxed{\frac{\partial}{\partial t}\vec{B}' = \vec{\nabla}\times\left[(\vec{U} - \varepsilon\vec{J})\times\vec{B}'\right] + \eta\nabla^2\vec{B}}\ , \qquad \vec{B}' = \vec{B} - \varepsilon_e^2\nabla^2\vec{B} - \frac{\varepsilon_e^2}{\varepsilon}\vec{\omega}$$

- Electron inertia is quantified by the dimensionless parameter $\varepsilon_e = \sqrt{\frac{m_e}{m_i}}\varepsilon = \frac{c}{\omega_{pe} L_0}$

- Just as the Hall effect introduces the new spatial scale $k_H = \frac{1}{\varepsilon}$ (the ion skin depth), electron inertia introduces the electron skin depth $k_e = \frac{1}{\varepsilon_e}$ which satisfies $k_e = \sqrt{\frac{m_i}{m_e}} k_H \gg k_H$

Normal modes in EIHMHD

- If we linearize our equations around an equilibrium characterized by a uniform magnetic field, we obtain the following dispersion relation:

$$\left(\frac{\omega}{\vec{k}\bullet\vec{B}_0}\right)^2 \pm \frac{k\varepsilon}{1+\varepsilon_e^2 k^2}\left(\frac{\omega}{\vec{k}\bullet\vec{B}_0}\right) - \frac{1}{1+\varepsilon_e^2 k^2} = 0$$

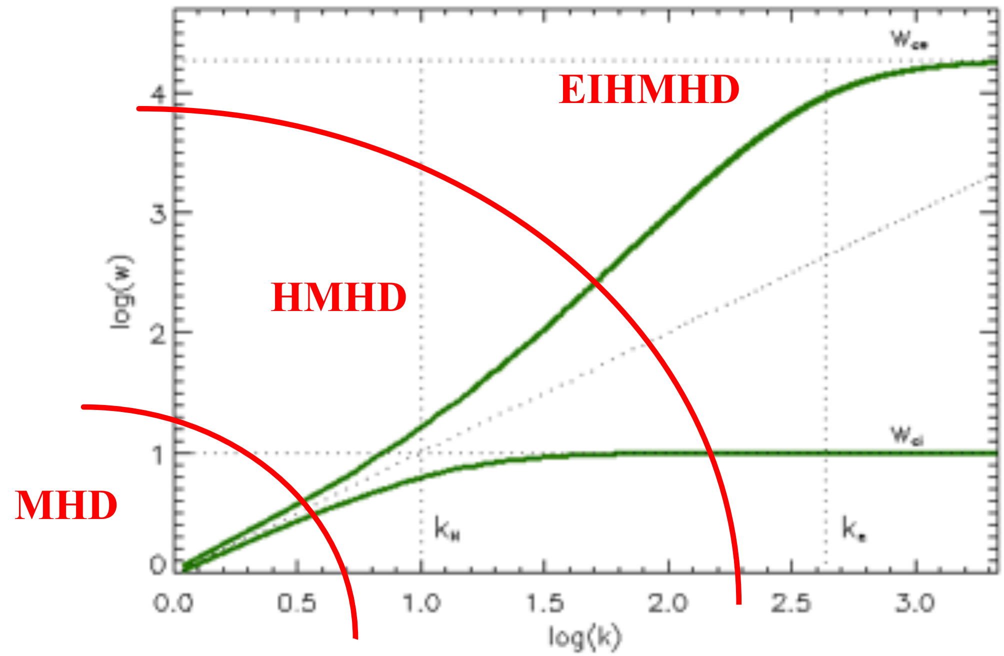

- Asymptotically, at very large k, we have two branches

$$\omega \xrightarrow[k\to\infty]{} \omega_{ce}\cos\theta$$

$$\omega \xrightarrow[k\to\infty]{} \omega_{ci}\cos\theta$$

while for very small k, both branches simply become Alfven modes, i.e.

$$\omega \xrightarrow[k\to 0]{} k\cos\theta$$

- Different approximations, just as one-fluid MHD, Hall-MHD and electron-inertia HMHD can clearly be identified in this diagram.

Ideal invariants in EIHMHD

- For each species s in the incompressible and ideal limit

$$m_s n_s \left(\partial_t \vec{U}_s - \vec{U}_s \times \vec{W}_s\right) = q_s n_s (\vec{E} + \frac{1}{c}\vec{U}_s \times \vec{B}) - \vec{\nabla}(p_s + m_s n_s \frac{U_s^2}{2})$$

- Using that $\vec{J} = \frac{c}{4\pi}\vec{\nabla}\times\vec{B} = \sum_s q_s n_s \vec{U}_s$ and $E = -\frac{1}{c}\partial_t \vec{A} - \vec{\nabla}\phi$

we can readily show that energy is an ideal invariant, where

$$E = \int d^3r \left(\sum_s m_s n_s \frac{U_s^2}{2} + \frac{B^2}{8\Pi} \right)$$

- We also have a helicity per species which is conserved, where

$$H_s = \int d^3r \left(\vec{A} + \frac{c m_s}{q_s}\vec{U}_s \right) \bullet \left(\vec{B} + \frac{c m_s}{q_s}\vec{W}_s \right)$$

First application: **Magnetic reconnection**

- The standard theoretical model for two-dimensional stationary reconnection is the so-called **Sweet-Parker model** (Parker 1958)

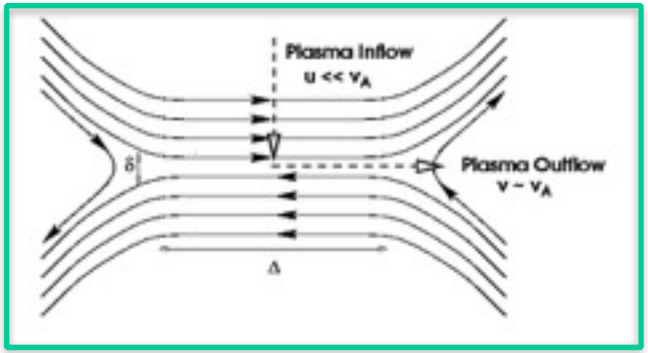

- It corresponds to a stationary solution of the MHD equations. The plasma inflow (from above and below) takes place over a wide region of linear size Δ and is much slower than the Alfven speed (i.e. $U_{in} << V_A$).

- The outflow occurs at a much thinner region (of linear size $\delta << \Delta$) at speed $U_{out} \sim V_A$.

- The efficiency of the reconnection process is measured by the so-called reconnection rate, which is the magnetic flux reconnected per unit time.

- The dimensionless reconnection rate is $$M = \frac{U_{in}}{U_{out}} \simeq S^{-1/2}$$

  where $S = \dfrac{\Delta v_A}{\eta}$ is the Lundquist number.

- Since for most astrophysical and space plasmas is S >> 1, the reconnection rate is exceedingly low.

EIHMHD simulations

- We perform simulations of the EIHMHD equations in 2.5D geometry to study magnetic reconnection. We force an external field with a double hyperbolic tangent profile to drive reconnection at two X points (Andres et al. 2014a, PoP).

- We also study the turbulent regime of the EIHMHD description, to look for changes at the electron skin-depth scale (Andres et al. 2014b, PoP).

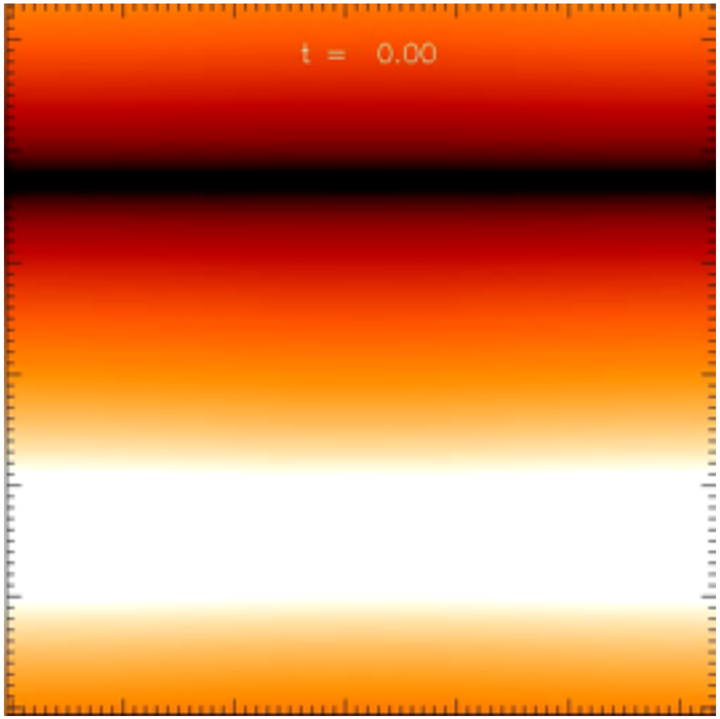

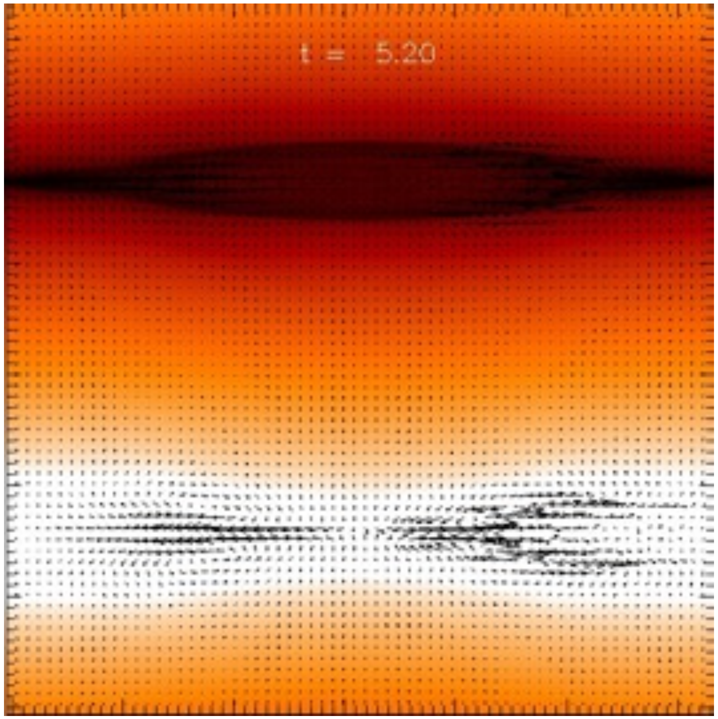

EIHMHD reconnection

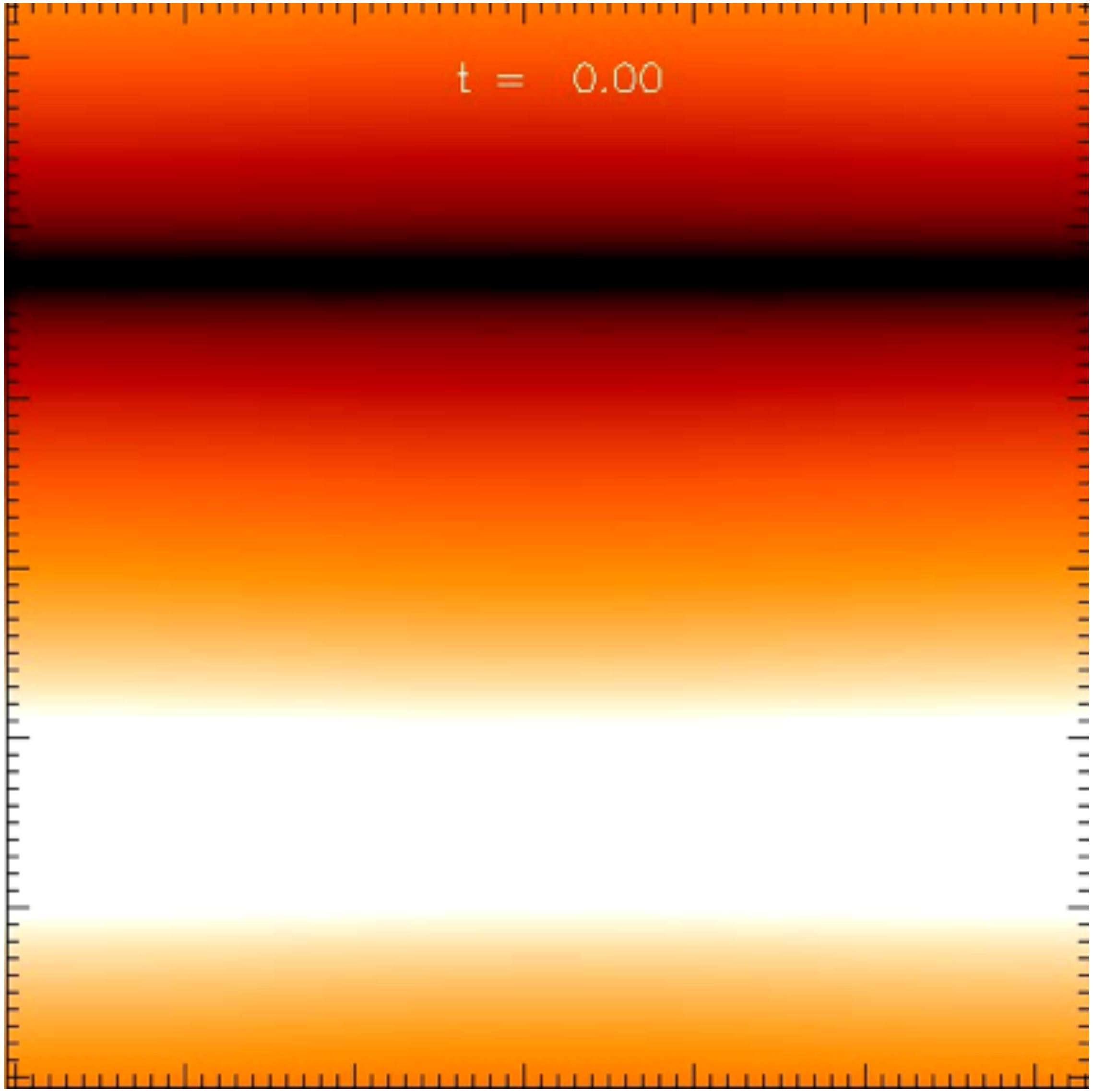

EIHMHD reconnection

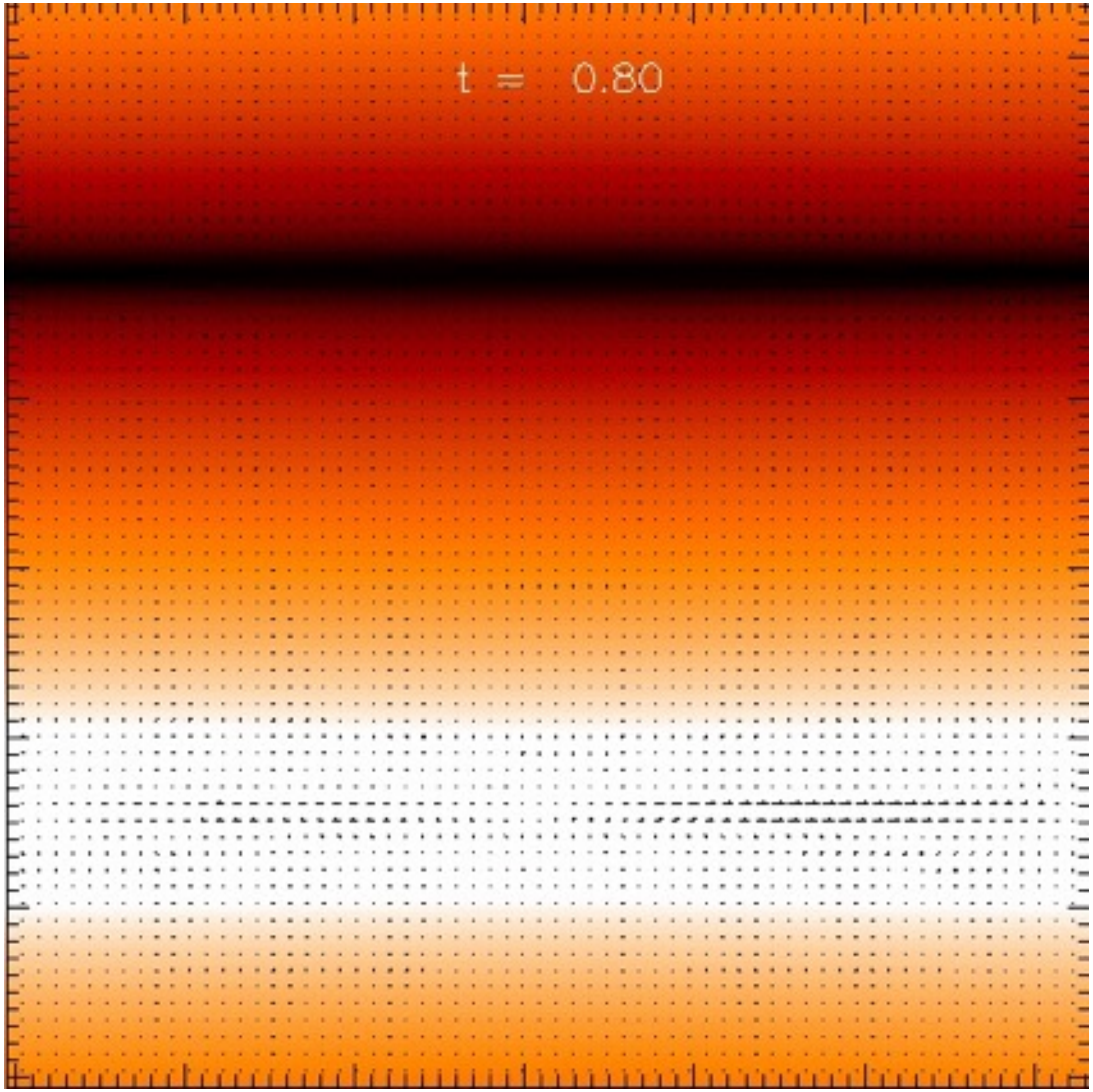

EIHMHD reconnection

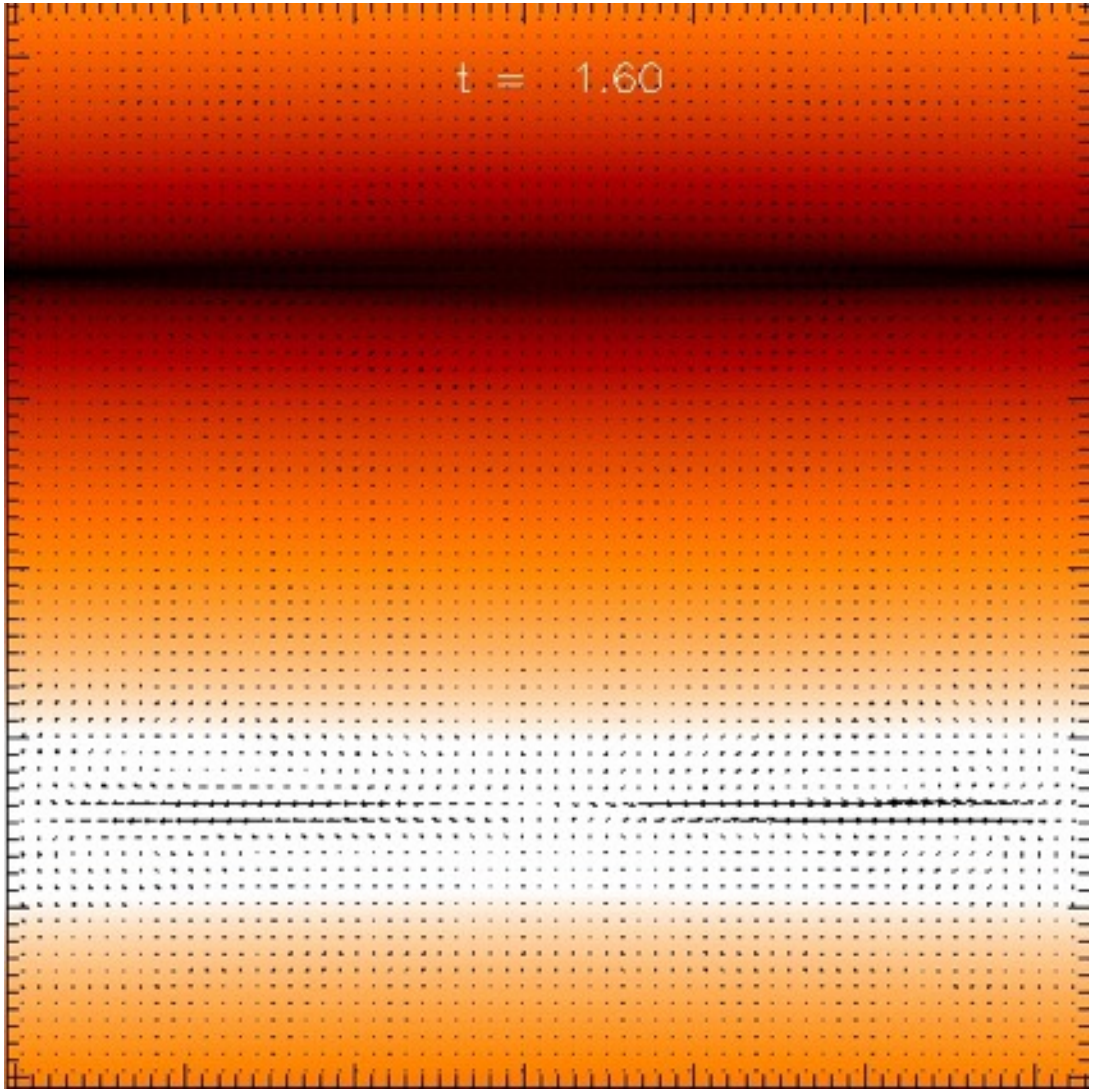

EIHMHD reconnection

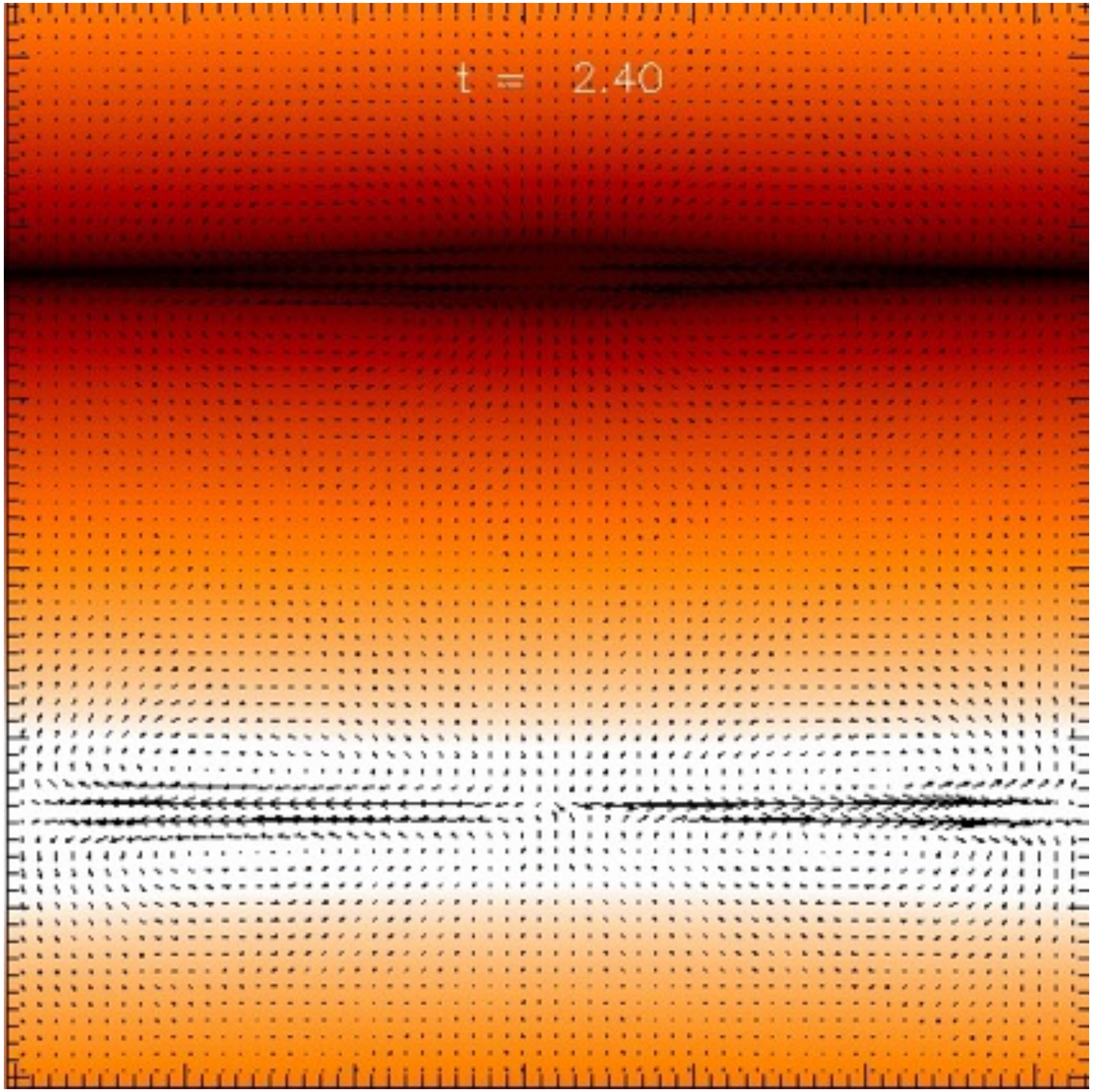

EIHMHD reconnection

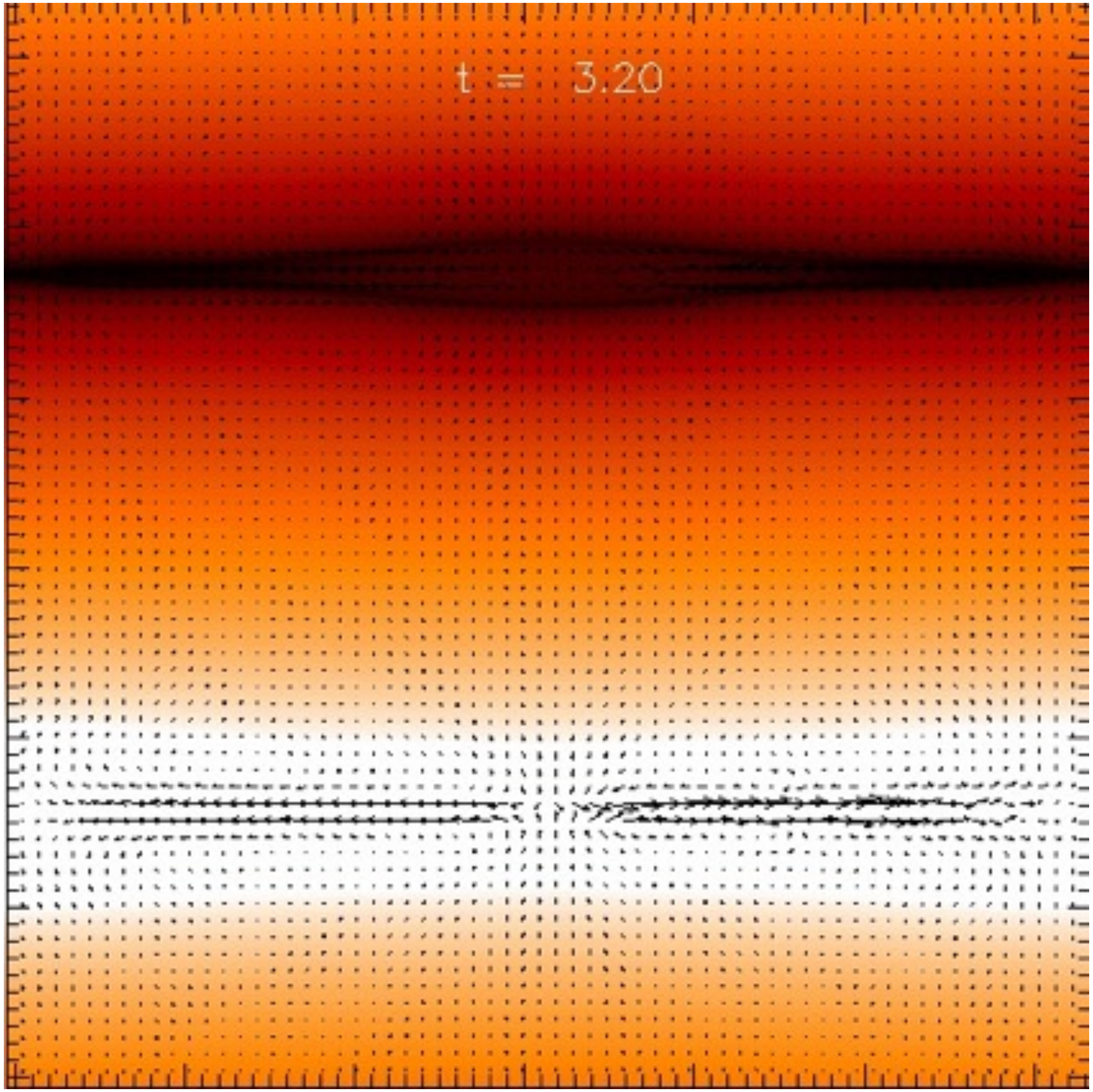

EIHMHD reconnection

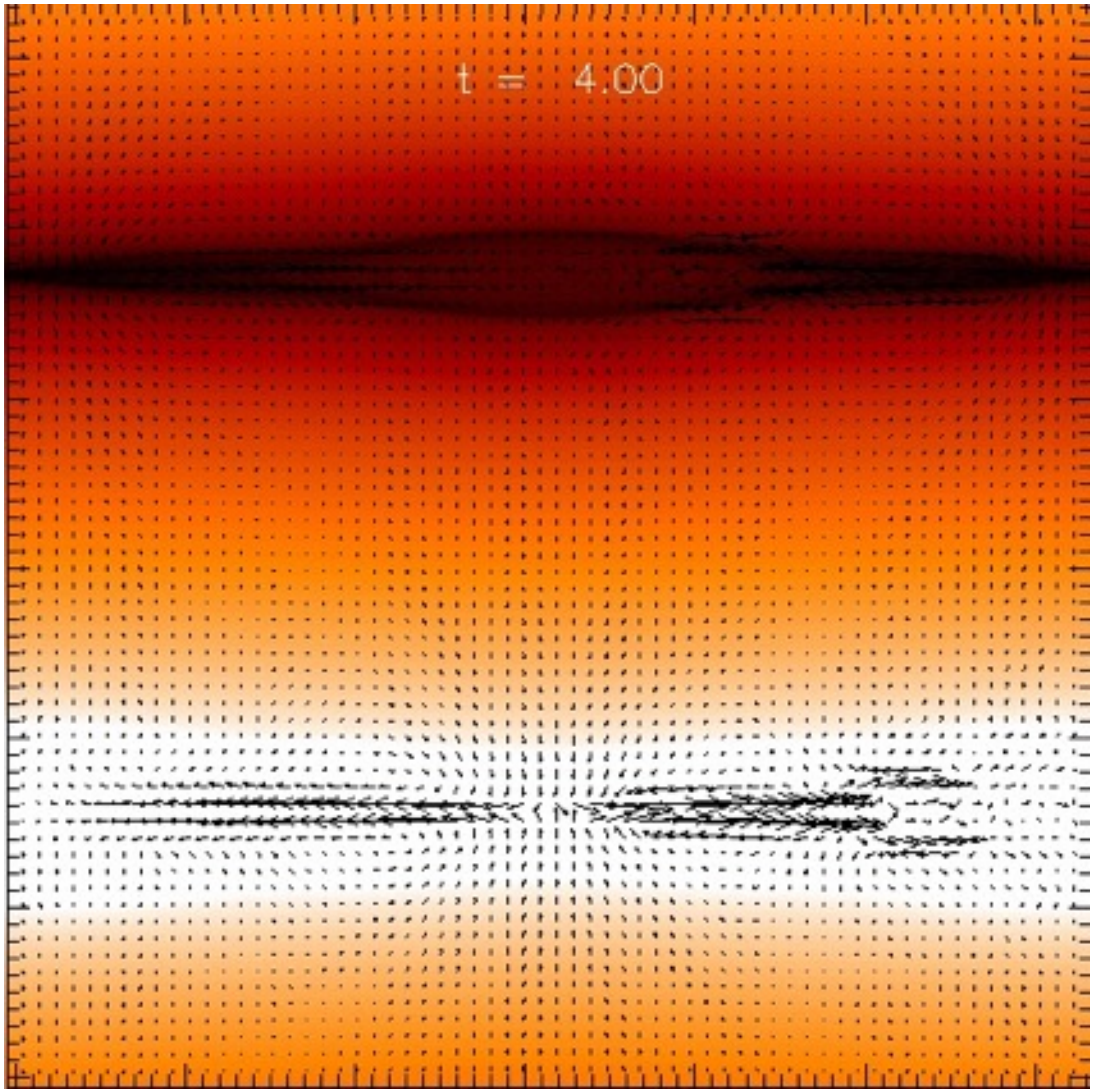

EIHMHD reconnection

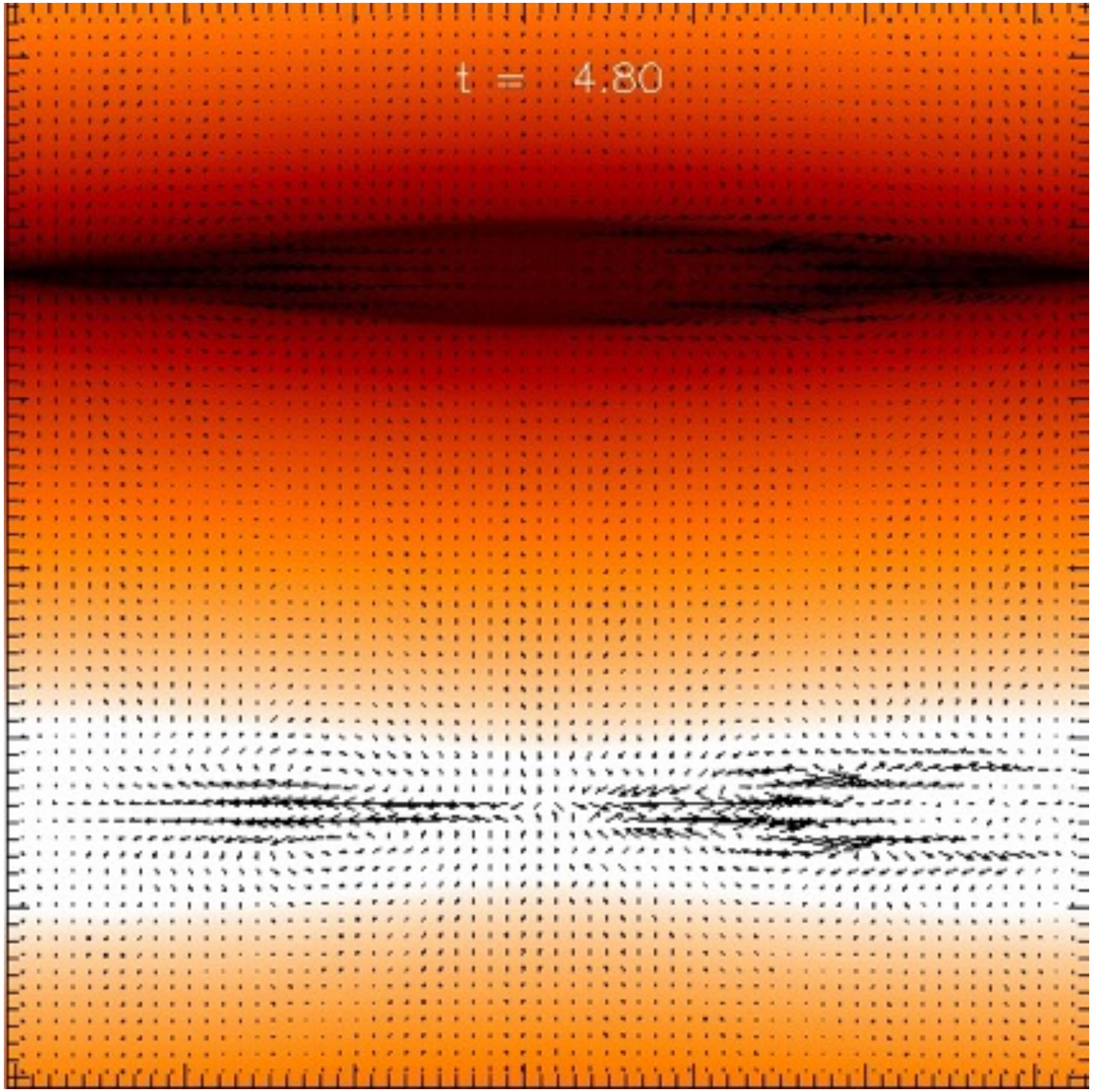

EIHMHD reconnection

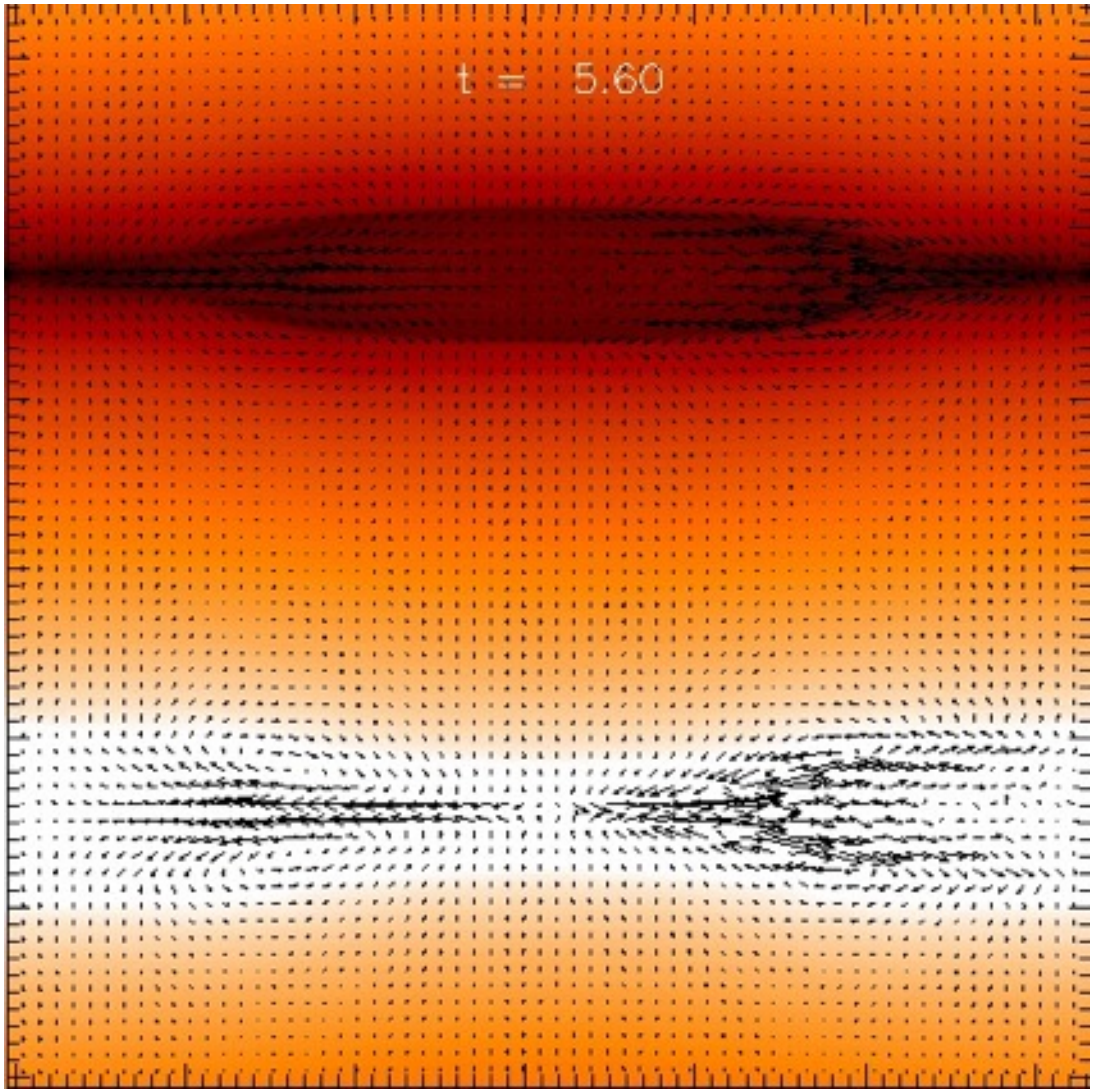

Reconnected flux in EIHMHD

- The total reconnected flux at the X-point is the magnetic flux through the perpendicular surface that extends from the O-point to the X-point.

- We compare the total reconnected flux between a run that includes electron inertia and another one that does not.

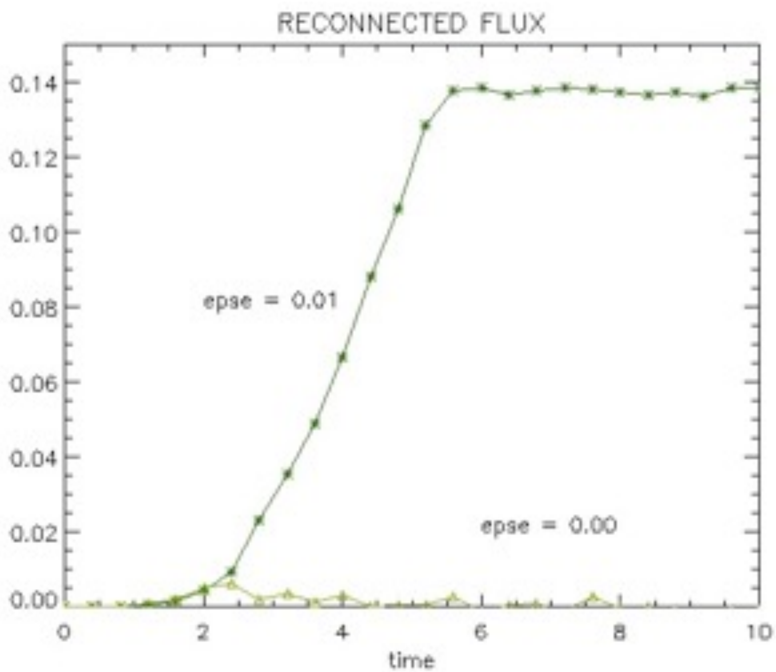

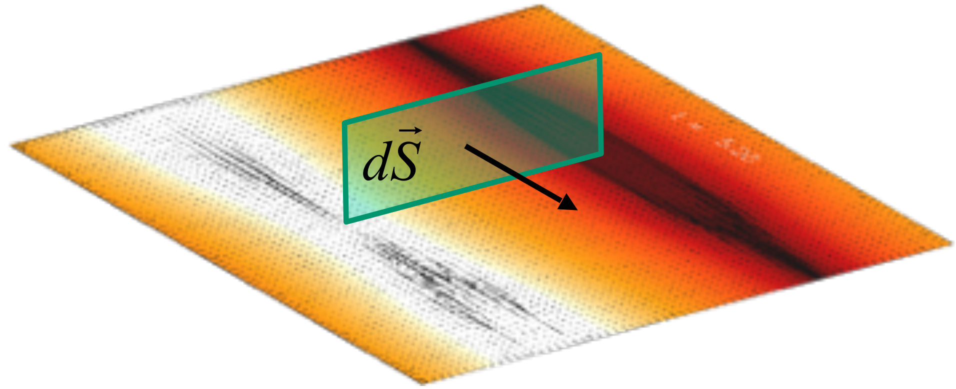

- The reconnection rate is the time derivative of these two curves.

- The apparent saturation is just a spurious effect stemming from the dynamical destruction of the X-point.

Reconnection rate in EIHMHD

- For the 2D configuration and assuming incompressibility, we run several simulations with different values of the Hall parameter, which is the dimensionless ion inertial length.
- We compare the corresponding reconnected flux (above) and the reconnection rate (below) vs. time.
- The reconnection rate is E_z at the X-point. From the equation for electrons, under stationary conditions

$$E_z = -\frac{m_e}{e}\hat{z}\cdot\vec{u}_e \times \vec{w}_e$$

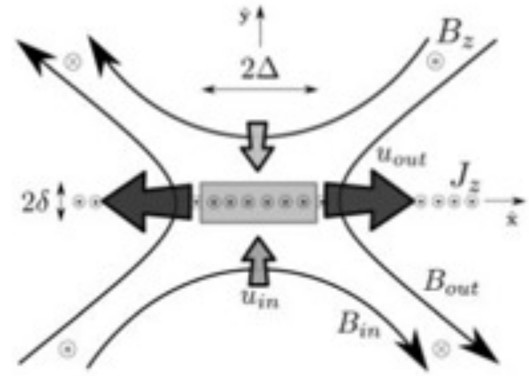

FIG. 1. Schematic 2.5D reconnection region.

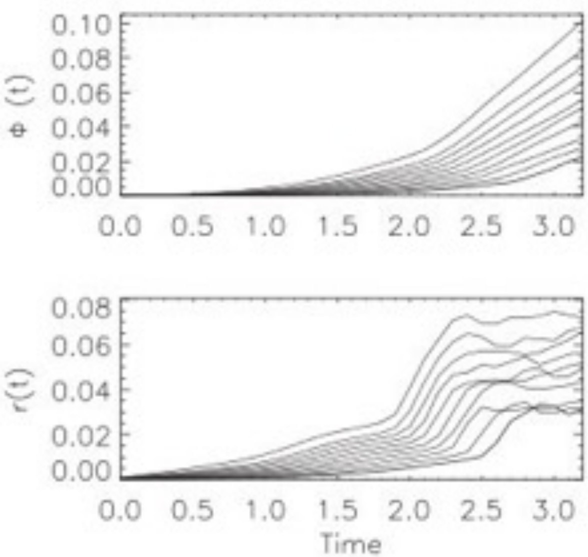

FIG. 3. Reconnected flux Φ (upper panel) and reconnection rate r (lower panel) as a function of time for $\lambda = 0.07, \ldots, 0.16$ (from bottom to top). For all runs, the electron to ion mass ratio is $m_e/m_i = 0.015$.

- At electron scales

$$\vec{u}_e \sim -\frac{1}{e\,n}\vec{j}$$

from where we obtain the following estimate for the dimensionless reconnection rate

$$R = \frac{c\,E_z}{B_0 v_A} \sim \frac{c}{w_{pi} L_0}$$

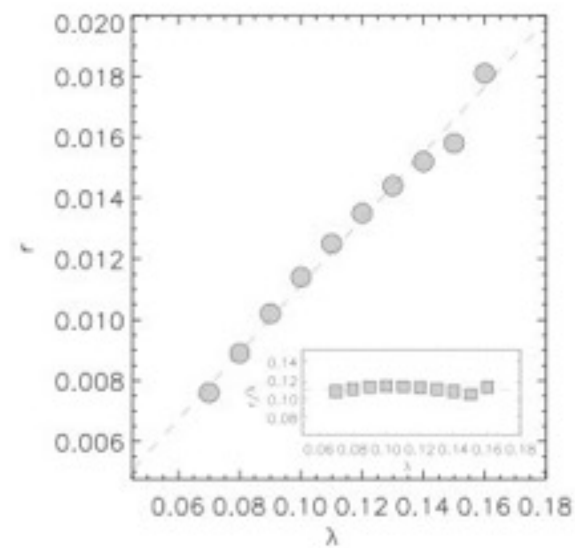

FIG. 6. Quasi-stationary reconnection rate r (gray circles) as a function of the Hall parameter λ. The best linear-fit for $\log\lambda - \log r$ is shown in gray-dashed line. Inset: Ratio between quasi-stationary reconnection rates and the Hall parameter (gray squares) as a function of the Hall parameter.

Second application: **Turbulence**

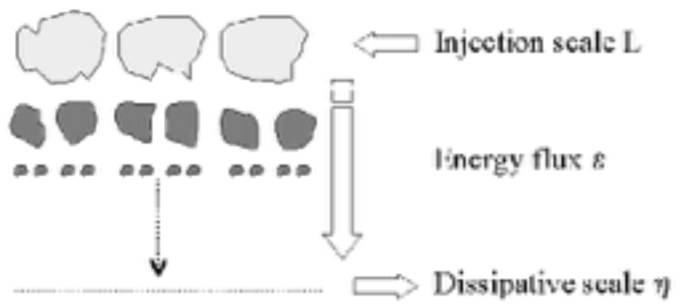

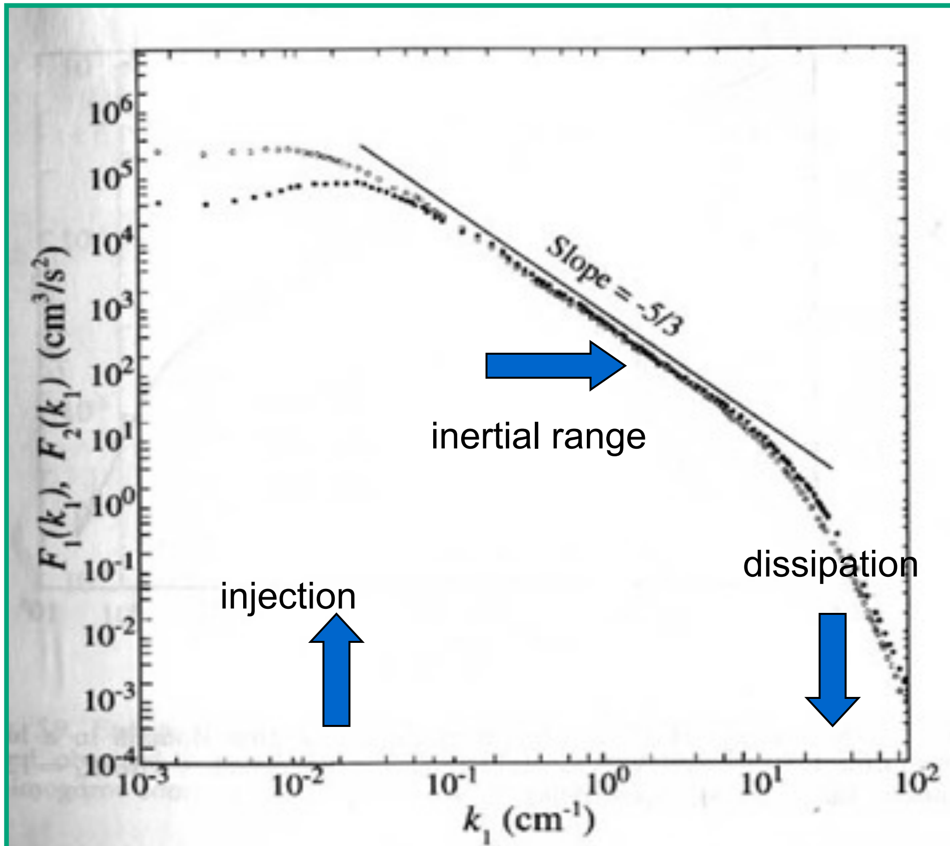

- Energy cascade
  - energy flux toward high k → $\varepsilon_k \approx \frac{u_k^2}{\tau_k}$
  - vortex breakdown

$$\tau_k \approx \frac{1}{ku_k}\ ,\ \varepsilon_k \approx \frac{u_k^2}{\tau_k} = const.$$

- Scale invariance
  - energy flux in k:
  - energy power spectrum: → $E_k \approx \frac{u_k^2}{k}$

- Therefore →

Kolmogorov spectrum (K41)

$$E_k \approx \frac{u_k^2}{k} = \varepsilon^{\frac{2}{3}} k^{-\frac{5}{3}}$$

Turbulence in the Solar Wind

- The **solar wind** is a stream of plasma released from the upper atmosphere of the Sun, which impacts and affects the planetary magnetospheres.
- Sahraoui et al. 2009 used magnetograms from the Cluster mission to derive power spectra of magnetic energy.

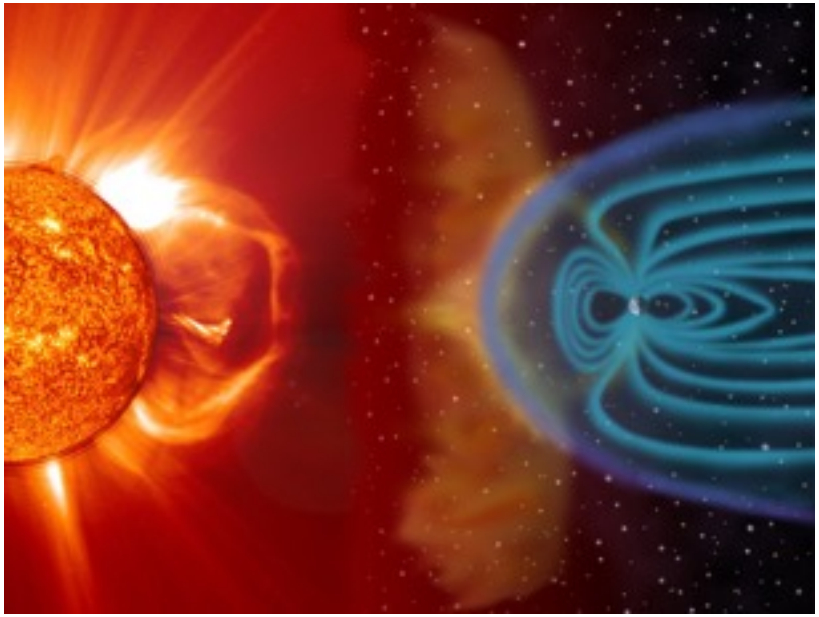

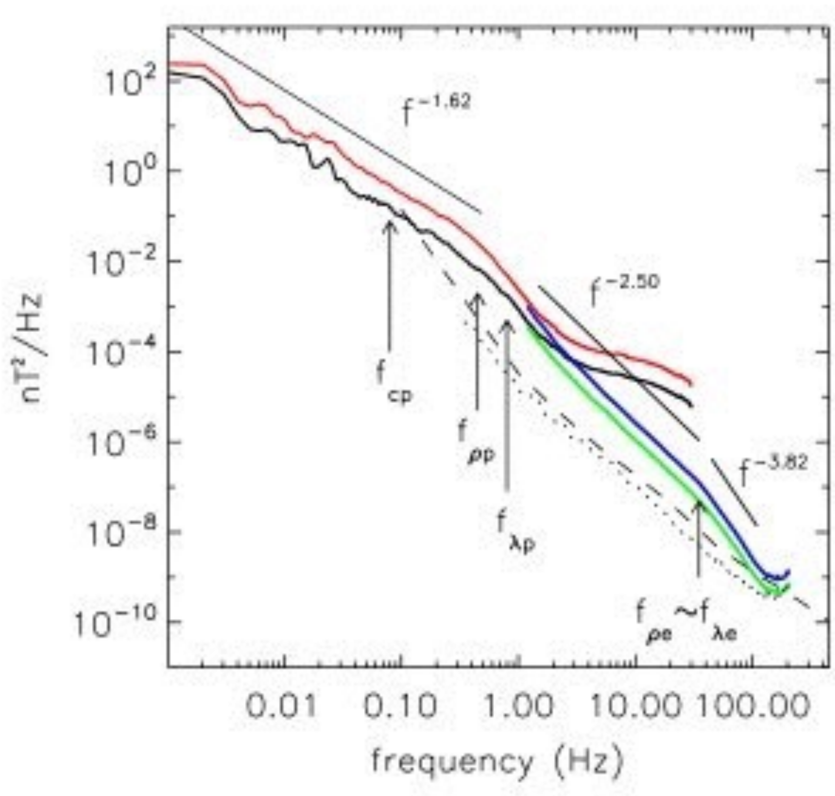

- They combine low-cadence data from FGM (**parallel** and **perpendicular** components) with high-cadence from STAFF-SC (also **parallel** and **perpendicular**).
- At the largest scales, they obtain a K41 power spectrum ($k^{-1.62}$).
- As they go to smaller scales, they identify two breakups. An intermediate range with a power law $k^{-2.50}$, and an even steeper range at the smallest scales ($k^{-3.82}$).

Turbulence in EIHMHD simulations

- These breakups are a manifestation of physical effects beyond MHD.
- We performed incompressible 3072x3072 simulations of the full two-fluid equations. We excited a ring of large-scale Fourier modes and let the system relax while the turbulent energy cascade takes place (Andres et al. 2014b, PoP).
- The magnetic energy power spectrum shows two breakups at the approximate locations of the proton (k_p) and electron (k_e) scales.

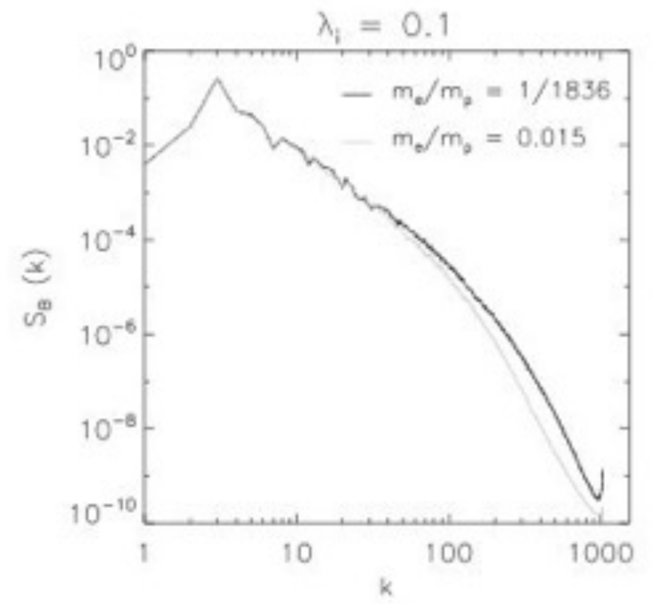

FIG. 1. Magnetic energy spectra for EIHMHD cases with $\lambda_i = 1/10$ and $m_e/m_p = 1/1836$ (black) and $m_e/m_p = 0.015$ (gray).

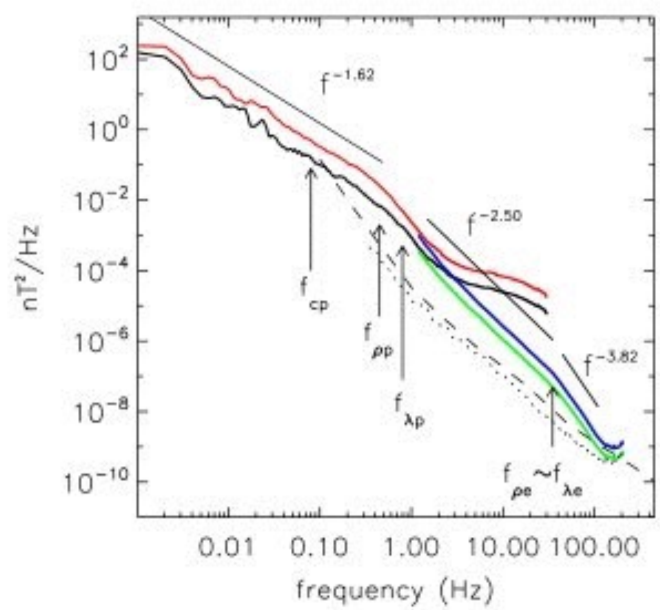

- The spectrum is K41 (i.e. $k^{-5/3}$) at $k << k_p$.
- At intermediate scales ($k_p << k << k_e$) is $k^{-7/3}$.
- Beyond the electron scale ($k_e << k$) a new range takes place $k^{-11/3}$.
- All these inertial ranges can be obtained using Kolmogorov-like arguments on the energy transfer rate given by

$$F_k \simeq k(u_k^3 + u_k B_k B'_k + (1-\delta)\lambda J_k B_k B'_k + (1-\delta)\delta\lambda^2 \partial_t J_k B_k).$$

Turbulence in EIHMHD simulations

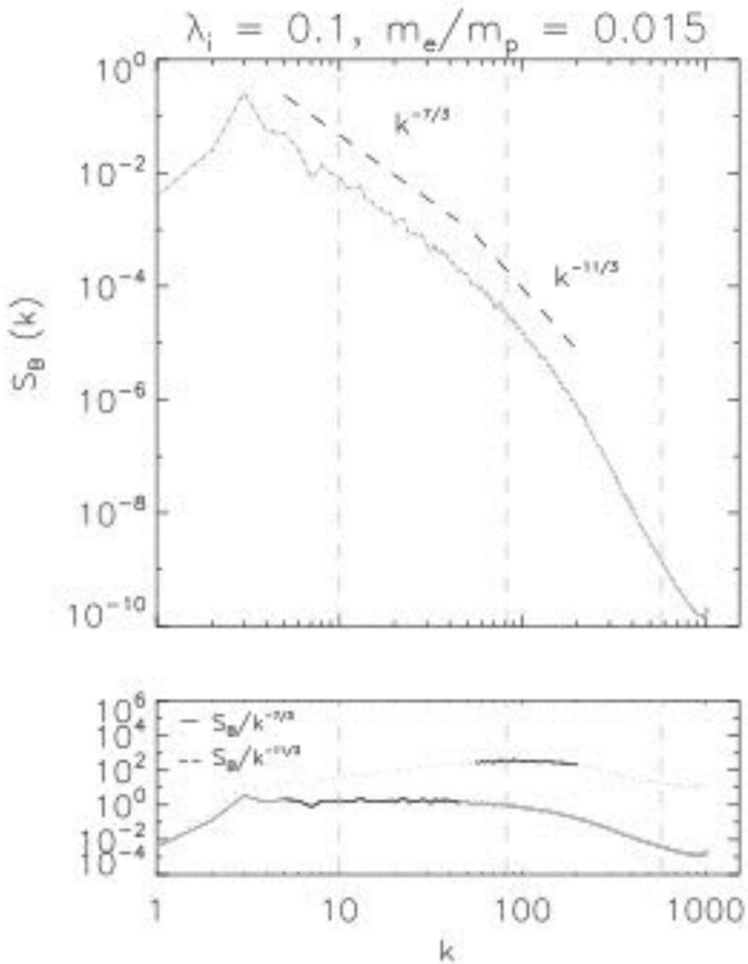

FIG. 2. Magnetic energy spectra for $m_e/m_p = 0.015$. Vertical dashed gray lines correspond to $k_{\lambda_i} \sim 10$, $k_{\lambda_e} \sim 82$, and $k_\nu \sim 550$. The compensated spectrum for the HMHD (solid line) and EIHMHD (dashed line) regions are shown in the lower panel.

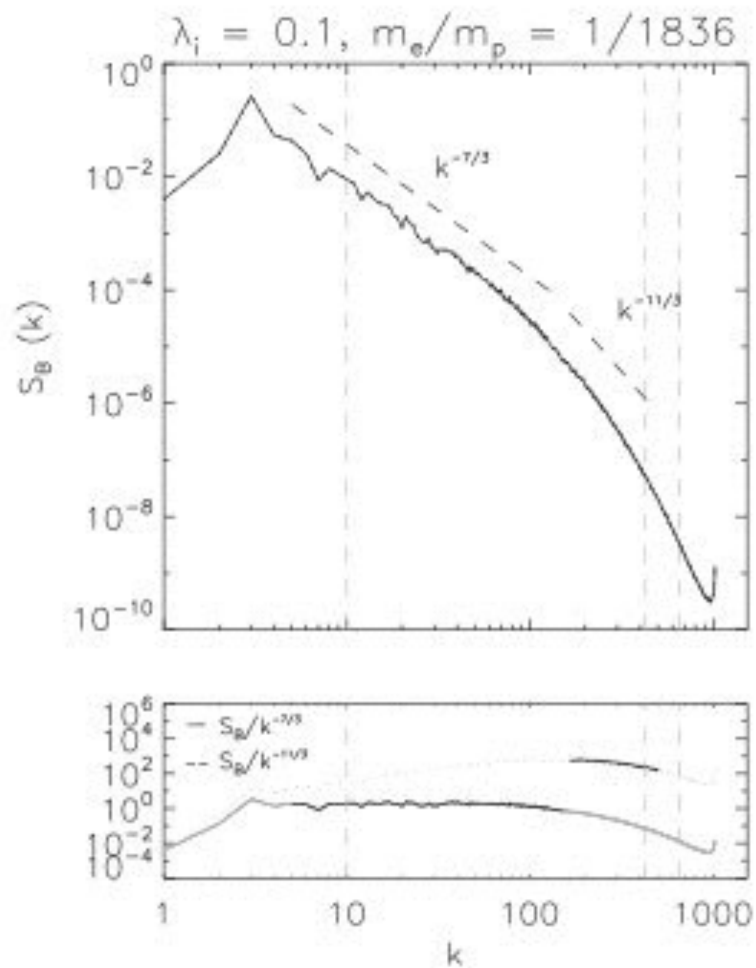

FIG. 3. Magnetic energy spectra for $m_e/m_p = 1/1836$. Vertical dashed gray lines correspond to $k_{\lambda_i} \sim 10$, $k_{\lambda_e} \sim 430$, and $k_\nu \sim 650$. The compensated spectrum for the HMHD (gray line) and EIHMHD (green line) regions in the same format as Figure 2.

Conclusions

- **One-fluid MHD** is a reasonable theoretical framework to describe the large-scale dynamics of plasmas.

- **Two-fluid MHD** introduces new physics (Hall, electron pressure, electron inertia) and also new spatial scales, such as the proton and electron skin-depths. We studied the role of these kinetic effects on two relevant phenomena for astrophysical plasmas: **reconnection** and **turbulence**.

- **Reconnection**:
  We present results from EIHMHD simulations to study dissipation-free magnetic reconnection. Our results show that it is indeed possible to have fast magnetic reconnection without energy dissipation (Andres et al. 2014a, PoP). The reconnection rate scales like the ion inertial scale and is independent from the electron mass.

- **Turbulence**:
  We also performed externally driven EIHMHD to show turbulent regimes. The magnetic energy spectrum displays breakups at the ion and electron inertial scales (Andres et al. 2014b, PoP). The spectral slopes are consistent with those arising from dimensional analysis.